Available online at www.sciencedirect.com
SCIENCE DIRECT®
Journal of Solid State Chemistry 177 (2004) 493–497
JOURNAL OF SOLID STATE CHEMISTRY
http://elsevier.com/locate/jssc

Structural materials: metal–silicon–Boron. The Nb-rich corner of the Nb–Si–B system

S. Katrych,[a,b] A. Grytsiv,[a,c] A. Bondar,[a] P. Rogl,[c] T. Velikanova,[a,*] and M. Bohn[d]

[a] *Frantsevich Institute for Problems of Materials Science of NASU, Krzhyzhanovsky Str.3, 03680 Kyiv, Ukraine*
[b] *Laboratory of Crystallography, Federal Institute of Technology, CH-8092 Zurich, Switzerland*
[c] *Institut für Physikalische Chemie, Universität Wien, Währingerstr. 42, A-1090 Wien, Austria*
[d] *UMR CNRS 6538, IFREMER, F-29263 Plouzané, France*

Received 2 December 2002; accepted 27 February 2003

Abstract

Phase equilibria in the Nb–Nb_5Si_3–NbB region were studied in the melting (crystallization) range by means of light microscopy, XRD, SEM and EMPA on alloys after arc-melting and annealing at 1800°C and at subsolidus temperatures. Phase transition and melting temperatures were determined by DTA and pyrometric Pirani–Alterthum technique resulting in a solidus projection and two isopleths, $Nb_{77}Si_{23}$–$Nb_{77}B_{23}$ and $Nb_{99}Si_1$–Nb_5Si_2B. The T_2-phase $Nb_5Si_{3-x}B_x$ ($0 \leqslant x \leqslant 2$, Cr_5B_3-type) was found to form equilibria with (Nb), NbB, Nb_3Si, and with the T_1-phase (Mn_5Si_3 derivative type). The T_2-phase melts incongruently ($Nb_5Si_{1.8}B_{1.2}$ at 2245°C) and forms a quasibinary eutectic with the niobium solid solution on a minimum tie-line at ~1880°C.

Keywords: Niobium silicon boride; B–Nb–Si phase diagram; Pseudobinary eutectic; Ternary phase

1. Introduction

Due to their high microhardness at room temperature and high yield stress and compressive strength at high temperatures, alloys NbB_2–Nb_5Si_3–$Nb_5Si_3B_2$ offer great potential as high-temperature structural materials [1,2]. Some restrictions in their application concerns their resistance to oxidation, which for the NbB_2–Nb_5Si_3–$Nb_5Si_3B_2$ alloys was believed to be higher than that for Nb_5Si_3 but lower than that for $NbSi_2$ [1]. The two-phase alloys (Nb) + Nb_5Si_2B are of interest since they are characterized by a disperse eutectic structure [3] that may be considered as an in situ metal–matrix composite.

Phase equilibria in the Nb–Si–B system were reported in detail at 1600°C by Nowotny et al. [4]. Detailed microstructure and XRD analyses were employed to construct the Nb–Nb_5Si_2B section [3] and the liquidus surface projection for Nb contents higher than 60 at% [5]. The authors of Ref. [3] claimed that alloys (Nb) + Nb_5Si_2B melt in a certain temperature interval above 2150°C, however, such high melting points are in contradiction to the liquidus projection proposed by Junior et al. [5] (not referring to melting point measurements), revealing a minimum in the monovariant liquidus lines connecting two binary invariant eutectic reactions: $L = (Nb) + NbB$ at 2170°C [6] and $L = (Nb) + Nb_3Si$ at 1915°C [7].

As melting points are of great importance in application of materials and in production technology, the main goals of the present work are the determination of melting points and the construction of the phase diagram for the Nb–Nb_5Si_3–NbB region at solidus temperatures.

2. Experimental procedure

The following starting materials were used: niobium bar (0.05 wt% Ta, 0.02 wt% Fe, less than 0.03 wt% N, less than 0.03 wt% C, less than 0.03 wt% O, 0.009 wt% Ti, and 0.009 wt% Si); monocrystalline semiconductor silicon (99.9999% Si); and boron powder (contained 5.3 wt% O, 0.055 wt% H, $\leqslant$0.1 wt% Cu, $\leqslant 10^{-2}$ wt% Fe, and $\leqslant 10^{-2}$ wt% Si), which was degassed by arc melting. The alloys were prepared from mixtures of Nb,

*Corresponding author.
E-mail address: velikanova@ipms.kiev.ua (T. Velikanova).

0022-4596/$ - see front matter © 2003 Elsevier Inc. All rights reserved.
doi:10.1016/j.jssc.2003.02.008

master-alloy $Nb_{51}B_{49}$, and Si by repeated arc-melting on a water-cooled copper hearth under Ti-gettered argon (pressure 50–80 kPa) with a nonconsumable tungsten electrode. The master-alloy contained 0.1 wt% oxygen and the impurity level in the alloys was about 0.05 wt% O, 0.04 wt% C, and less than 0.005 wt% N. The cooling rate of the samples was about 100°C/s. Weight losses were checked to be less than 0.8% and nominal compositions were adopted after chemical analysis of selected alloys.

Temperatures of phase transformation were determined by DTA using HfO_2 crucibles and W/W-20Re thermocouples under high-purity helium with heating and cooling rates of 0.5°C/s. The melting points were measured after the Pirani and Alterthum method by use of an optical pyrometer with instrumental errors of ± 4°C for the temperature range from 1400°C to 2000°C and ± 12°C for the range from 2000°C to 3000°C. After first observation of melting, samples were annealed for 30–60 min at about 10–30°C below melting. Melting points were registered several times and the samples were finally re-annealed for 60 min followed by cooling at a rate of 150–200°C/s. Some alloys were annealed for 4 h at 1800°C in Hf-gettered argon, followed by furnace cooling.

As-cast and annealed samples were examined by powder X-ray diffraction (XRD) using a Guinier–Huber image plate system with Cu$K\alpha_1$ radiation (internal standard of 99.9999 wt% pure Ge with $a = 0.5657906$ nm). Scanning electron microscopy and quantitative compositions were determined on a CAMEBAX SX-50 electron-beam probe microanalyzer.

3. Binary boundary systems

Crystal data for the binary and ternary solid phases of the Nb–Nb_5Si_3–NbB region are presented in Refs. [4,6–8]. A recent thermodynamic modeling of the Nb–Si phase diagram by Fernandes et al. [9] is based on the assessment of Ref. [7] showing the $\alpha \leftrightarrow \beta$ polymorphic transformation of Nb_5Si_3 in the temperature range 1645–1935°C (from Cr_5B_3 to W_5Si_3 structure types, respectively). Nb_3Si is proposed to exist in the temperature range from 1765°C to 1975°C. The Nb–B phase diagram is accepted after Ref. [6], which is mainly based on Ref. [10]. In this version the (Nb) + NbB eutectic is at 19 at% B, 2170°C and Nb_3B_2 forms in a solid reaction at 2080°C.

4. Results and discussion

Alloy compositions and results are summarized in Table 1 and Figs. 1–6.

Table 1
Composition and melting temperatures of Nb–Si–B alloys

Alloy composition (at%)			XRD data on phase composition of annealed alloys	DTA melting point[a] (°C)	Solidus temperature[b] after Pirani and Alterthum (°C)				Temperature of subsolidus annealing (°C)
Nb	Si	B			T	Δ_{stat}	Δ_{tot}	n	
81.5	17.5	1	(Nb) + T_2	1920	1894	2	6	9	1880
67	31	2		1910	1897	3	6	6	1885
77	21	2		1920	1904	4	7	7	1870
77	18	5		1920	1891	4	7	7	1880
77	13	10		1890	1913	11	12	10	1900
62.5	36	1.5	T_2	>2100[c]	2250	(45)	(45)	3	1830
62.5	22.5	15		>2100[c]	1871[d]	12	13	16	1825
					245			2	
77	5	18	(Nb) + NbB + T_2[e]	2000	2011	2	12	10	1990
59	5	36		1990	2005	5	13	9	1985
60	15	25	T_2 + NbB	>2100[c]	2237	13	19	4	1920
57.5	17.5	25	NbB + T_1 + T_2	>2100[c]	2246	8	15	9	2165
80	20	—	(Nb) + Nb_3Si + $\alpha Nb_5Si_3(T_2)$	1935	—	—	—	—	—
62	38	—	$\alpha Nb_5Si_3(T_2)$ + T_1[f]	>2100[c]	2302	21	25	8	1820

[a] Temperature after DTA was measured on the annealed samples.
[b] Δ_{stat} and Δ_{tot}—statistical and total errors of measured temperature, n—number of measurements.
[c] No melting was observed up to maximal temperature used for DTA (2100°C).
[d] Melting of non-equilibrium (Nb) + T_2 eutectic.
[e] Phase composition of as cast samples (after subsolidus annealing forth phase Nb_3B_2 was appeared).
[f] In this alloy, the T_1-phase (its content is close to a XRD detection threshold) was attributed to stabilization of interstitial contamination, ~0.05 wt% O and ~0.04 wt% C.

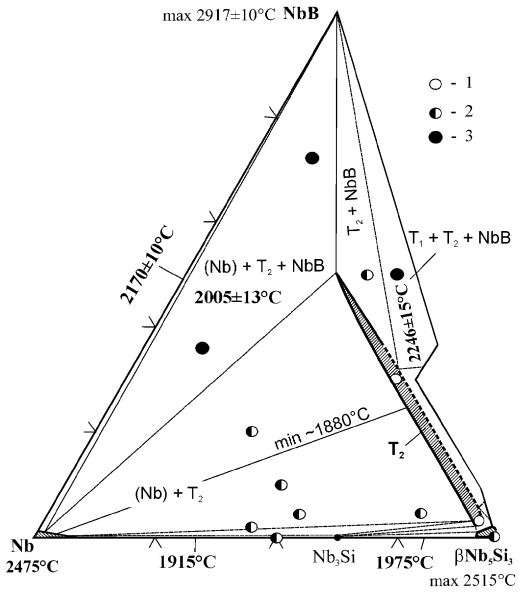

Fig. 1. Solidus surface projection for the Nb–Nb_5Si_3–NbB region: (1) single phase samples after annealing; (2) two-phase samples; and (3) three-phase samples.

The character of phase equilibria at subsolidus temperatures differs only little from those at 1600°C [4], and there are no inconsistencies with the liquidus projection proposed by Junior et al. [5]. At solidus temperatures there exist the same two ternary phases as in the 1600°C isothermal section, which are denoted as T_1 (derivative from the Mn_5Si_3 structure type) and T_2 (Cr_5B_3 structure type). As a consequence of the substitution of Si by B the phase T_2 is considered to be a ternary extension of isostructural binary αNb_5Si_3. The maximum substitution of Si by B, established from EPMA and lattice parameter data ($Nb_{66}Si_{11}B_{23}$, $Nb_{64}Si_{13}B_{23}$, and $Nb_{63}Si_{12}B_{25}$ for the 77Nb–5Si–18B and 59Nb–5Si–36B (at%) alloys), corresponds to the stoichiometric composition Nb_5SiB_2 (Fig. 1). Thus the T_2-phase essentially is a line compound $Nb_5Si_{3-x}B_x$ (where $0 \leqslant x \leqslant 2$) with lattice parameters monotonically decreasing from binary αNb_5Si_3 (Fig. 2). The melting temperature of T_2 was found to be about 2250°C (see Table 1) by Pirani–Althertum measurement of the 62.5Nb–22.5Si–15B and 62.5Nb–36Si–1.5B (at%) alloys. Both alloys were multi-phase in as-cast state: $T_2 + T_1 + \mathrm{NbB} + (\mathrm{Nb})$ and $T_2 + T_1$ (traces), but they

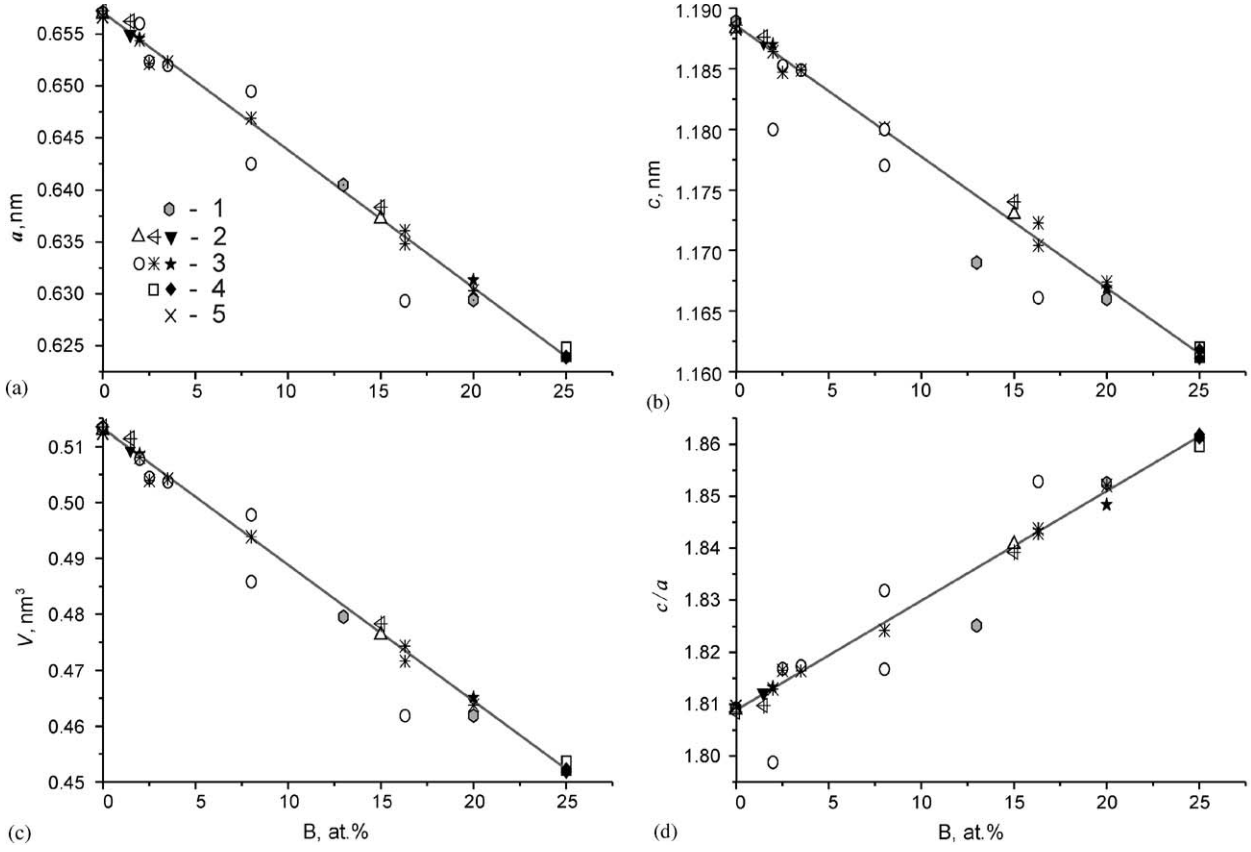

Fig. 2. The composition dependence of the T_2-phase lattice parameters: (1) binary phase αNb_5Si_3 [7] and ternary T_2-phase from Refs. [3,4]; (2) single phase alloys, as-cast and annealed at subsolidus temperatures and 1800°C; (3) two-phase alloys (Nb) + T_2 and T_2 + NbB, as-cast and annealed at subsolidus temperatures and 1800°C; (4) EMPA and XRD data for the alloys (Nb) + NbB + T_2, as-cast and annealed at subsolidus temperatures; and (5) as-cast alloy 80Nb–20Si (at%).

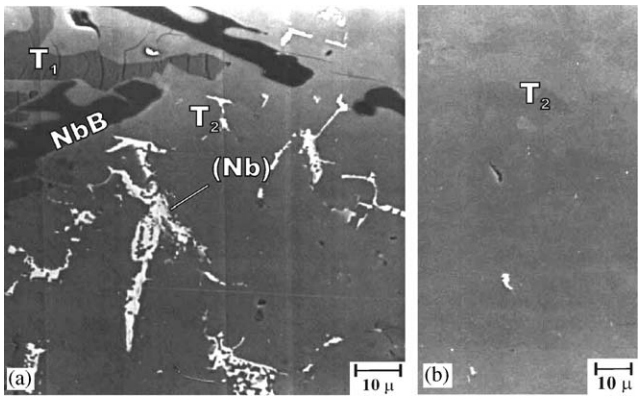

Fig. 3. Microstructure of alloy $Nb_{62.5}Si_{22.5}B_{15}$: (a) 62.5Nb–22.5Si–15B (at%), as-cast; and (b) annealed at 1825°C.

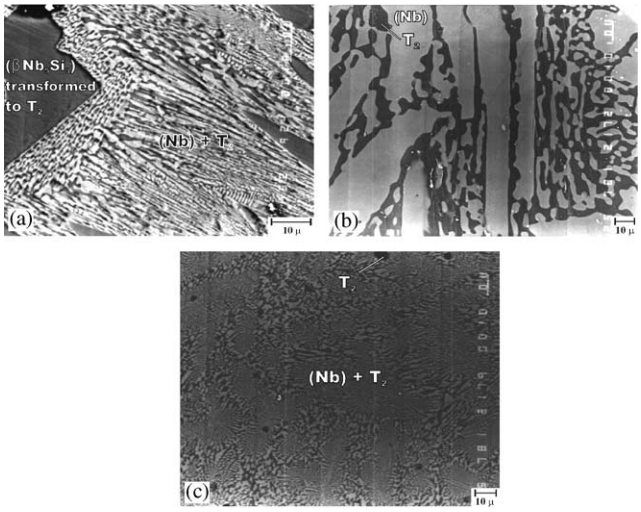

Fig. 4. Microstructure of two-phase alloys (Nb) + T_2: (a) 67Nb–31Si–2B (at%), as-cast; (b) annealed at 1885°C; and (c) 77Nb–13Si–10B (at%), as-cast.

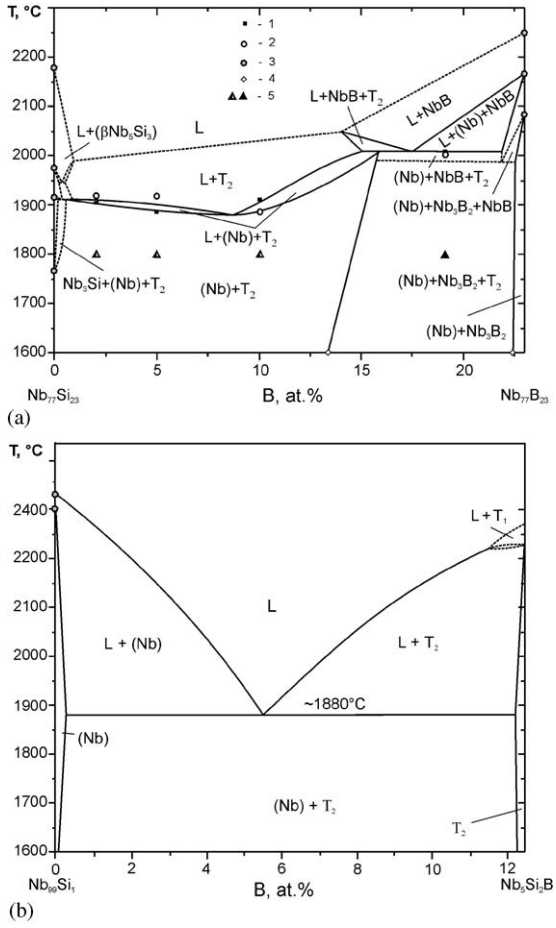

Fig. 5. Vertical sections $Nb_{77}B_{23}$–$Nb_{77}Si_{23}$ (a) and $Nb_{99}Si_1$–Nb_5Si_2B (b). (1) Melting point after Pirani–Alterthum; (2) DTA thermal arrests; (3) binary phase diagram data [6,7]; (4) data from the 1600°C isothermal section [4]; and (5) two-phase and three-phase samples annealed at 1800°C.

became single phase after annealing (Fig. 3). XRD reflections from the T_2 lattice in the annealed alloy 62.5Nb–36Si–1.5B (at%) are split, confirming suggestions that T_2 forms by a dual mechanism: either from liquid or due to a solid-state transformation $\beta Nb_5Si_3 \rightarrow \alpha Nb_5Si_3(T_2)$ in cooling. Such a behavior is explained by the narrow temperature stability range of βNb_5Si_3 under solidus temperatures resulting in difficulties to quench this phase from temperatures below solidus. Accordingly transformed βNb_5Si_3 can be easily observed in as-cast alloys as primary crystallized parallelepipeds (Fig. 4a), but it disappears in cooling or annealing at 25°C below solidus (Fig. 4b) to form T_2.

Special attention should be paid to the two-phase alloys (Nb) + T_2, which contain a highly dispersed eutectic (Fig. 4c). This large phase field is characterized by a shallow minimum on the ruled solidus surface, so that its location is difficult to be determined precisely (Fig. 5a). The minimum eutectic tie-line, (Nb) + T_2, seems to be at a temperature of about 1880°C between the alloy compositions 77Nb–13Si–10B and 77Nb–18Si–5B (at%) close to the vertical section $Nb_{99}Si_1$–Nb_5Si_2B (Fig. 5b). The melting points obtained on the (Nb) + T_2 alloys are at considerably lower temperature than those of Ref. [3], who reported a temperature higher than 2150°C for alloys of the Nb–Nb_5Si_2B section. Although the section $Nb_{99}Si_1$–Nb_5Si_2B includes the tie-line with the quasibinary eutectic within the precision of data obtained, it cannot be considered as strictly quasibinary owing to incongruent melting at the boundary compositions $Nb_{99}Si_1$ and Nb_5Si_2B.

Due to the extended region (Nb) + T_2 at solidus temperatures, the phase fields involving Nb_3Si (Ti_3P structure type) are very close to the Nb–Si side. That is why Nb_3Si was observed neither in ternary as-cast alloys nor in annealed alloys. Whilst Nb_3Si is easily identified in the XRD pattern of the binary as-cast alloy 80Nb–20Si (at%), its decomposition is not observed in the DTA curves (Fig. 6a).

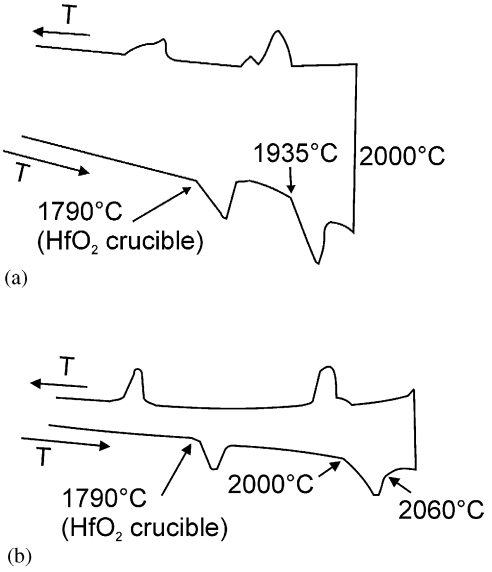

Fig. 6. DTA curves for alloys: (a) as-cast 80Nb–20Si (at%) and (b) 77Nb–5Si–18B (at%) annealed at 1990°C. (The thermal arrests at around 1790°C correspond to the transformation in HfO_2-crucible.)

The obtained EMPA data reveal a small solubility of about 0.1–0.3 at% silicon in NbB (CrB structure type). The (Nb) phase contains up to 2.1 at% Si as derived from the alloy 67Nb–31Si–2B (at%) annealed at 1910°C.

The study of the phase relations involving the T_1-phase, which is a derivative from the Mn_5Si_3 structure type, will be the subject of future activities. The T_1-phase is confirmed to be stable in the subsolidus temperature range (including 1800°C) in the vicinity of its stochiometry Nb_5Si_3B. The melting temperatures for the three-phase field $T_1 + T_2 + NbB$ on the solidus surface was determined to be at 2246 ± 15°C.

In the present work the Nb_3B_2 boride (U_3Si_2 structure type) was not detected in as-cast alloys, but alloys from the (Nb) + NbB + T_2 field, annealed at subsolidus temperature (Table 1), showed four phases (Nb) + Nb_3B_2 + NbB + T_2. Taking into consideration the fact that melting points in the fields (Nb) + Nb_3B_2 + T_2 and Nb_3B_2 + T_2 + NbB are almost equal, we believe that Nb_3B_2 is absent on the Nb–Si–B solidus surface. DTA curves (Fig. 6b) do not reveal any evidence for the formation of Nb_3B_2, which therefore seems to be rather sluggish.

5. Conclusion

The phase diagram in the Nb–Nb_5Si_3–NbB region is characterized by an extended homogeneity range of the αNb_5Si_3–Nb_5SiB_2 solid solution (T_2-phase), which melts incongruently. The T_2-phase forms equilibria with all the phases in the region studied: (Nb), Nb_3Si, βNb_5Si_3, NbB and T_1-phase on the solidus surface. The section $Nb_{99}Si_1$–Nb_5Si_2B includes the quasibinary eutectic, $L \Leftrightarrow (Nb) + T_2$, on a minimum tie-line at $\sim$1880°C.

Acknowledgments

S.K. is grateful to the OEAD and to the University of Vienna for stipends in Vienna. The authors thank Mr. V.M. Petiukh for the DTA experiments.

References

[1] T. Murakami, C.N. Xu, A. Kitahara, M. Kawahara, Y. Takahashi, H. Inui, M. Yamaguchi, Intermetallics 7 (1999) 1043–1048.
[2] T. Murakami, A. Kitahara, M. Kawahara, Y. Takahashi, H. Inui, M. Yamaguchi, in: High-temperature ordered intermetallic alloys VIII, Mat. Res. Soc. Symp. Proc. Vol. 552, Mater. Res. Soc., Warrendale, PA, USA, pp. KK8.26.1–KK8.26.6.
[3] K.C.G. Candioto, C.A. Nunes, G.C. Coelho, P.A. Suzuki, Mater. Characterization 47 (2001) 241–245.
[4] H. Nowotny, F. Benesovsky, E. Rudy, A. Wittmann, Monatsch. Chemie. 91 (1960) 975–990.
[5] D.M.P. Junior, C.A. Nunes, G.C. Coelho, F. Ferreira, Intermetallics 11 (2003) 251–255.
[6] P. Rogl, in: G. Effenberg (Ed.), Phase Diagrams of Ternary Metal–Boron–Carbon Systems, ASM-MSI, Materials Park, OH, USA, 1998, p. 205.
[7] M.E. Schlesinger, H. Okamoto, A.B. Gokhale, R. Abbaschian, J. Phase Equilibria 14 (1993) 502–509 (see also J. Phase Equilibria 16 (1995) 296).
[8] T.B. Massalski, P.R. Subramanian, H. Okamoto (Eds.), Binary Alloys Phase Diagrams, ASM International, Materials Park, OH, USA, 1990.
[9] P.B. Fernandes, G.C. Coelho, F. Ferreira, C.A. Nunes, B. Sundman, Intermetallics 10 (2002) 993–999.
[10] E. Rudy, Compendium of phase diagram data, Air Force Materials Laboratory, Wright-Patterson AFB, OH, USA, 1969, p. 206.